

Enhancing model estimation accuracy and convergence rate in hysteresis modeling of MFC actuators using modified differential evolution algorithm

Hafiz Muhammad Umar¹, Ruichen Yu², Zhiyuan Gao³, Hesheng Zhang⁴

School of Mechatronic Engineering and Automation, Shanghai University, Shanghai, 200444, China

³Corresponding author

E-mail: ¹hafizumar0725@outlook.com, ²shuyrc99@shu.edu.cn, ³gaozhiyuan86@163.com,

⁴zhs81@shu.edu.cn

Received 6 April 2023; accepted 29 April 2023; published online 18 May 2023

DOI <https://doi.org/10.21595/vp.2023.23309>



63rd International Conference on Vibroengineering in Shanghai, China, May 18, 2023

Copyright © 2023 Hafiz Muhammad Umar, et al. This is an open access article distributed under the Creative Commons Attribution License, which permits unrestricted use, distribution, and reproduction in any medium, provided the original work is properly cited.

Abstract. This paper presents a study on improving the estimation accuracy and convergence rate of hysteresis modeling of MFC actuators using mutation enhanced differential evolution (MEDE) algorithm, a modified version of the differential evolution algorithm. The proposed MEDE algorithm uses three mutation strategies, i.e., best, rand, and pbest. To model the secondary path of a smart flexible beam with MFC actuators, a Hammerstein model that combines an asymmetric Bouc-Wen model with an ARX model connected in series is proposed. The fitness function values of the Hammerstein model are compared with evolutionary algorithms.

Keywords: ARX model, asymmetric Bouc-Wen model, Hammerstein model, MFC actuators, mutation enhanced differential evolution algorithm.

1. Introduction

MFC is a popular piezocomposite transducer with high-performance characteristics, widely used in various applications [1]. However, the performance of MFC actuator is limited by its nonlinear and hysteretic behavior [2].

Bouc-Wen model is popular for describing hysteresis nonlinearity of piezoelectric materials [3-5], but it can only account for symmetric hysteresis. Since MFC actuators exhibit asymmetric hysteresis, alternative model needs to be developed. Wang Geng [6] suggested a modified Bouc-Wen (MBW) model to capture the asymmetric hysteresis nonlinearity of the piezoelectric actuator. Since the actual hysteretic nonlinear curve of MFC actuator is related to rate. To tackle the aforementioned challenge, one approach is to connect the hysteretic nonlinear model in series with a linear model, resulting in a Hammerstein model [7]. For example, Konstantinos Krikelis proposed a Hammerstein model that integrates the Prandtl-Ishlinskii hysteresis model with a linear recursive neural network [8].

The aim is to enhance the model estimation accuracy and convergence rate in hysteresis modeling of MFC actuators without explicitly identifying the model parameters. Instead of identifying the model parameters, we use the fitness function output, including fitnessbestX, favg, fmax, fmin, and fstd, to compare the performance of different optimization algorithms. In this study, the MEDE algorithm based on multiple mutation strategies is used to optimize the fitness of the proposed Hammerstein model. Section 2 provides a detailed description of the proposed Hammerstein model. Section 3 presents the methodology for applying the MEDE algorithm. The results are presented in Section 4. Section 5 finally describes the conclusion.

2. Model for hysteresis characterization in MFC actuators

2.1. Bouc-Wen hysteresis model

A classical Bouc-Wen model defined by the following equations, can characterize the dynamic behavior of MFC actuators [9, 10]:

$$Z(t) = M\ddot{x}(t) + D\dot{x}(t) + Kx(t) = K[Lu(t) - h(t)], \quad (1)$$

$$\dot{h}(t) = \alpha L\dot{u}(t) - \beta|\dot{u}(t)|h(t) - \gamma\dot{u}(t)|h(t)|, \quad (2)$$

where, the linear Eq. (1) relating the input voltage (u) to the output displacement (h) and nonlinear differential Eq. (2) describing the displacement change over time. α , β and γ are hysteresis loop parameters; M , D , K and L are the mass, damping coefficient, stiffness and piezoelectric coefficient respectively. It can describe symmetric hysteresis due to its assumption that the nonlinearity is symmetric about the origin. This mathematical formulation results in symmetric hysteresis loops for both loading and unloading cycles as shown in Fig. 1. The Bouc-Wen model is specifically designed to account for the hysteresis phenomenon, which is a characteristic property of MFC actuators.

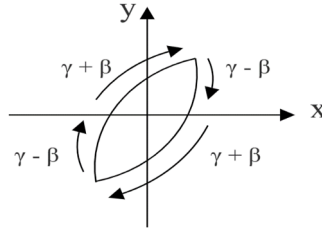


Fig. 1. Symmetry of Bouc-Wen model

$Z(t)$ is made up of two components: a hysteretic component $Kh(t)$ with memory and non-hysteretic component $p(t) = KLu(t)$ without memory. As a result $Z(t) = p(u(t)) - Kh(t)$.

2.2. Asymmetric Bouc-Wen model in discrete form

The MFC actuator exhibits asymmetric hysteresis, so the model needs to improve. This paper proposes a modification in Eq. (1) of the classical Bouc-Wen model with the non-hysteretic component $p(t)$ to the polynomial $p(u(t))$:

$$p(u(t)) = d_1u(t) + d_2u^2(t), \quad (3)$$

where, d_1 and d_2 are the parameters. Thus, the asymmetric Bouc-Wen model can be given by:

$$Z(t) = M\ddot{x}(t) + D\dot{x}(t) + Kx(t) = K_1u(t) + K_2u^2(t), \quad (4)$$

$$\dot{h}(t) = \alpha L\dot{u}(t) - \beta|\dot{u}(t)|h(t) - \gamma\dot{u}(t)|h(t)|. \quad (5)$$

Before being employed in digital control systems, the asymmetric Bouc-Wen model must be discretized. As a result, we use the Laplace transform and bilinear transform, as shown below:

$$r(K) = -\frac{1}{e_1} [f_1r(K-1) + g_1r(K-2) - eh_1(K) - fh_1(K-1) - gh_1(K-2)], \quad (6)$$

$$h_1(K) = d_1u(K) + d_2u^2(K) - h(K), \quad (7)$$

$$h(K) = \alpha Lu(K) - \beta|u(K)|h(K-1) - \gamma u(K)|h(K-1)| + h(K-1). \quad (8)$$

From the Eq. (6); $e = T_s^2$, $f = 2T_s^2$, $g = T_s^2$, $e_1 = 4M + 2DT_s + KT_s^2$, $f_1 = 2KT_s^2 - 8M$, $g_1 = 4M - 2DT_s + KT_s^2$. The variable T_s denotes the sample time.

2.3. Development of a Hammerstein model for improved modeling of MFC actuators

To improve the model of MFC actuators further, a novel approach using a Hammerstein model that combines a discrete asymmetric Bouc-Wen model with a linear component with dynamic behavior is proposed. The model accounts for the rate-dependent hysteresis nonlinearity of MFC actuators. The proposed model comprises two modules: a static nonlinear component represented by the asymmetric Bouc-Wen model, and a dynamic linear component represented by the ARX model. The input signal first passes through the static nonlinearity block, which captures the actuator’s asymmetric behavior. The output of this block is then fed into the linear dynamic system block, which is modeled using a second-order ARX model as shown in Fig. 2. The ARX model is as follows:

$$Q(z) = \frac{r_1(z)}{r(z)} = \frac{az^{-1} + bz^{-2}}{cz^{-1} + dz^{-2} + 1}, \tag{9}$$

$$r_1(K) = ar(K - 1) + br(K - 2) - cr_1(K - 1) - dr_1(K - 2), \tag{10}$$

where, a , b , c and d are the parameters of an ARX model.

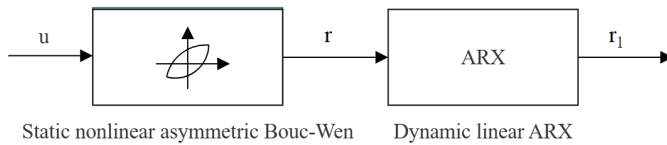


Fig. 2. Proposed Hammerstein model structure

3. Methodology

3.1. The traditional differential evaluation (DE) algorithm

DE algorithm is a widely used optimization method belonging to evolutionary algorithms family. It involves maintaining a population of candidate solutions and improving them iteratively by combining their features [11]. It is divided into the following parts:

3.1.1. Initialization

To initialize the DE algorithm, a population of target vectors of size NP is generated. Each target vector is a row vector of dimension D , denoted as $X_{i,G} = \{x_{1,G}, x_{2,G}, x_{3,G}, \dots, x_{NP,G}\}$. X_{min} and X_{max} represent the lower and upper bounds of the solution space for each dimension. A common method is to generate initial population using a uniform distribution where each element is generated as $X_{i,j} = X_{min} + rand(0,1) * (X_{max} - X_{min})$, where j ranges from 1 to D ; $rand(0,1)$ is a random number between 0 and 1.

3.1.2. Mutation

The DE algorithm mutates the current population to generate new candidate solutions. The mutation operator perturbs a target vector $X_{i,G}$ to create a mutant vector $V_{i,G}$ using a customizable parameter called, mutation factor denoted as mF . The mutation techniques are presented as [12].

DE / rand/ 1:

$$V_{i,G} = X_{a_1,G} + mF * (X_{a_2,G} - X_{a_3,G}). \tag{11}$$

DE / best / 1:

$$V_{i,G} = X_{best,G} + mF * (X_{a_1,G} - X_{a_2,G}). \quad (12)$$

DE / current-to-best / 1:

$$V_{i,G} = X_{i,G} + mF * (X_{best,G} - X_{i,G}) + mF * (X_{a_1,G} - X_{a_2,G}), \quad (13)$$

where, $X_{a_1,G}$, $X_{a_2,G}$, and $X_{a_3,G}$ are three randomly selected base vectors, a_1 , a_2 , and a_3 are indices of different vectors in the population, and $a_1 \neq a_2 \neq a_3 \neq i$. $X_{best,G}$ is the best vector in the population. Mutation factor mF is a positive value normally varies between 0 and 2.

3.1.3. Crossover

Crossover, combine the mutant vector with the target vector. The crossover operation randomly selects a dimension of the mutant vector and replaces it with the corresponding dimension of the target vector to form a trial vector. The binomial crossover as follows:

$$H_{i,G}^j = \begin{cases} V_{i,G}^j, & rand_j \leq CR \text{ or } j = j_{rand}, \\ X_{i,G}^j, & \text{otherwise,} \end{cases} \quad (14)$$

where, CR is a positive value between 0 and 1, $rand_j \in [0, 1]$ is a uniform random number, and j_{rand} is a randomly selected index within the range of dimensions of the vectors.

3.1.4. Selection

In selection, each candidate vector competes with its corresponding target vector based on their fitness value. The most common selection method in DE algorithm is the greedy selection, as follows:

$$X_{i,G+1} = \begin{cases} H_{i,G}, & f(H_{i,G}) \leq f(X_{i,G}), \\ X_{i,G}, & \text{otherwise,} \end{cases} \quad (15)$$

where, $f(H_{i,G})$ and $f(X_{i,G})$ are the objective functions to be minimized.

3.2. The mutation enhanced differential evolution (MEDE) algorithm

The MEDE algorithm is a modified version of the DE algorithm, which incorporates multiple mutation strategies and a dynamic mutation factor range. The multiple mutation strategies allow the algorithm to explore different regions of the search space simultaneously, while the dynamic mutation factor range helps to balance the global and local search abilities of the algorithm. Each individual in the population is mutated using one of the three mutation strategies: 'best', 'rand', or 'current-to-pbest' selected randomly. 'best' uses the best solution identified so far as the base vector, 'rand' uses a randomly selected solution as the base vector, and 'current-to-pbest' uses a set of pbest solutions and a randomly selected solution as the base vector. The modified mutation factor and mutation strategies describe as follows:

$$mF = F_{min} + rand() * (F_{max} - F_{min}). \quad (16)$$

DE / best / 1:

$$V_{i,G} = X_{best,G} + mF * (X_{a_1,G} - X_{a_2,G}). \quad (17)$$

DE / rand / 1:

$$V_{i,G} = X_{a_1,G} + mF * (X_{a_2,G} - X_{a_3,G}). \quad (18)$$

DE / current-to-pbest / 1:

$$V_{i,G} = X_{i,G} + mF * (X_{pbest,G} - X_{i,G}) + mF * (X_{a_1,G} - X_{a_2,G}), \quad (19)$$

where, F_{min} and F_{max} are the lower bound and upper bound mutation factors respectively. $X_{pbest,G}$ is picked at random as one of the top 100p% of the present population with $p \in (0, 1]$. The MEDE algorithm can be used to optimize in case of fitness of Hammerstein. The fitness function for a proposed model, can be expressed mathematically as:

$$f = \sum_{n=1}^l (s_{exp}^n - s_{model}^n)^2, \quad (20)$$

where s_{exp} is the measured output, s_{model} is the predicted output. The smaller the fitness function value, the closer the match between the predicted output and the actual experimental data.

4. Experimental setup and results

4.1. Experiment setup

The experimental platform utilized in this study is an active vibration control (AVC) experimental platform built in the Advanced Perception and Control laboratory, Shanghai University. It consists of a robust cantilever beam system equipped with MFC actuators and sensors, along with a power amplifier, charge amplifier, target PC, and host PC. The MFC actuators used were M5628-P2, while the sensors used were M0714-P2. Fig. 3 presents a photo of the experimental setup, which was captured by our team in February 2023.

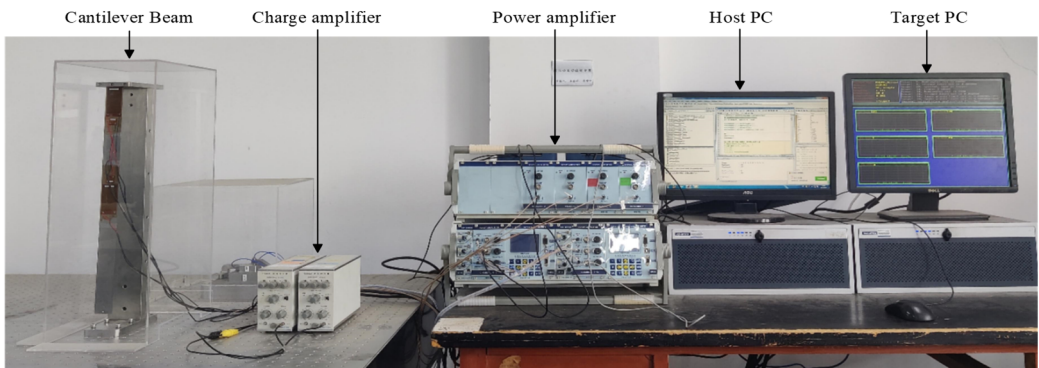


Fig. 3. Experimental setup for the cantilever beam system

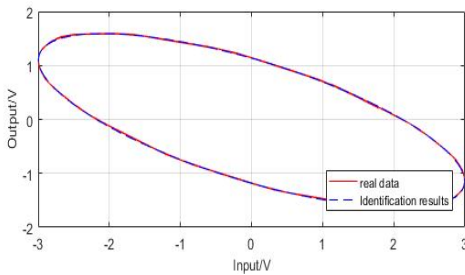
4.2. Results

Table 1 displays the results.

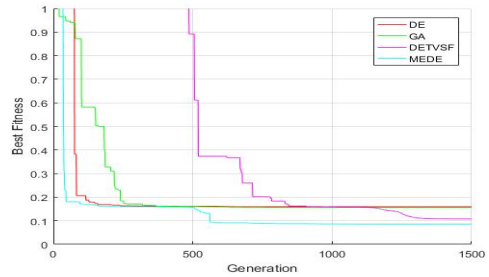
Table 1. Fitness function results

Algorithms	Best fitness value	f_{avg}	f_{max}	f_{min}	f_{std}	Iteration (xx)
DE	0.1596	0.2055	5.1557	-1.0198	0.8903	100
GA	0.1565	0.3082	1.000	$1.3339e^{-13}$	0.3616	100
DETVSF	0.1083	-0.3767	69.8311	-8.4037	2.8881	100
MEDE	0.0860	0.8026	75.6401	-8.5651	8.0847	100

Fig. 4(a) compares the hysteresis curves of real data (actual experiment) with identification findings (Hammerstein model). Fig. 4(b) compares the greatest fitness value for various algorithms. MEDE’s best fitness value is more consistent with the experimental response than DE, GA, and DETVSF. As a result, the proposed MEDE algorithm produces significantly superior results.



a) Hysteresis curve comparison



b) Best fitness value comparison

Fig. 4. Comparison of real data and identification results hysteresis curves and best fitness values

5. Conclusions

This paper proposes an improved hysteresis model that combines an asymmetric Bouc-Wen model with an ARX model connected in series to form a Hammerstein model and an optimization algorithm called MEDE. The proposed model accurately describes the Hammerstein hysteresis loop, while the MEDE algorithm optimizes the model’s performance. The comparison of MEDE with other algorithms shows that it provides more satisfactory optimal performance in terms of the fitness function.

Acknowledgements

This work is supported by National Natural Science Foundation of China (Grant Nos. 52175101, 61503232).

Data availability

The datasets generated during and/or analyzed during the current study are available from the corresponding author on reasonable request.

Conflict of interest

The authors declare that they have no conflict of interest.

References

- [1] J. Zhou, J. Zhou, W. Chen, J. Tian, J. Shen, and P. Zhang, “Macro fiber composite-based active and efficient suppression of low-frequency vibration of thin-walled composite beam,” *Composite Structures*, Vol. 299, p. 116019, Nov. 2022, <https://doi.org/10.1016/j.compstruct.2022.116019>

- [2] M. S. Rana, H. R. Pota, and I. R. Petersen, "Nonlinearity effects reduction of an AFM piezoelectric tube scanner using MIMO MPC," *IEEE/ASME Transactions on Mechatronics*, Vol. 20, No. 3, pp. 1458–1469, 2015.
- [3] M. Salah and A. Saleem, "Hysteresis compensation-based robust output feedback control for long-stroke piezoelectric actuators at high frequency," *Sensors and Actuators A: Physical*, Vol. 319, p. 112542, Mar. 2021, <https://doi.org/10.1016/j.sna.2021.112542>
- [4] X. Xue, X. Wu, L. Chen, and Q. Sun, "Bouc-Wen modeling to hysteresis nonlinear in macro fiber composite (MFC) actuator," *International Journal of Applied Electromagnetics and Mechanics*, Vol. 45, No. 1-4, pp. 965–971, May 2014, <https://doi.org/10.3233/jae-141931>
- [5] Y.-L. Yang, Y.-D. Wei, J.-Q. Lou, L. Fu, G. Tian, and M. Wu, "Hysteresis modeling and precision trajectory control for a new MFC micromanipulator," *Sensors and Actuators A: Physical*, Vol. 247, pp. 37–52, Aug. 2016, <https://doi.org/10.1016/j.sna.2016.05.027>
- [6] G. Wang, G. Chen, and F. Bai, "Modeling and identification of asymmetric Bouc-Wen hysteresis for piezoelectric actuator via a novel differential evolution algorithm," *Sensors and Actuators A: Physical*, Vol. 235, pp. 105–118, Nov. 2015, <https://doi.org/10.1016/j.sna.2015.09.043>
- [7] L. Yang, Z. Zhao, Y. Zhang, and D. Li, "Rate-dependent modeling of piezoelectric actuators for nano manipulation based on fractional hammerstein model," *Micromachines*, Vol. 13, No. 1, p. 42, Dec. 2021, <https://doi.org/10.3390/mi13010042>
- [8] K. Krikelis, K. van Berkel, and M. Schoukens, "Artificial neural network hysteresis operators for the identification of hammerstein hysteretic systems," *IFAC-PapersOnLine*, Vol. 54, No. 7, pp. 702–707, 2021, <https://doi.org/10.1016/j.ifacol.2021.08.443>
- [9] Royson D. D. 'Souza, Bineesh Benny, Anil Sequeira, and Navin Karanth P., "Hysteresis modeling of amplified piezoelectric stack actuator for the control of the microgripper," *American Scientific Research Journal for Engineering, Technology, and Sciences*, Vol. 15, No. 1, pp. 265–281, Jan. 2016.
- [10] M. Nafea M., Z. Mohamed, A. M. Abdullahi, M. R. Ahmad, and A. R. Husain, "Dynamic hysteresis based modeling of piezoelectric actuators," *Jurnal Teknologi*, Vol. 67, No. 5, Mar. 2014, <https://doi.org/10.11113/jt.v67.2834>
- [11] S. Das, S. S. Mullick, and P. N. Suganthan, "Recent advances in differential evolution – An updated survey," *Swarm and Evolutionary Computation*, Vol. 27, pp. 1–30, Apr. 2016, <https://doi.org/10.1016/j.swevo.2016.01.004>
- [12] G. Sun, B. Yang, Z. Yang, and G. Xu, "An adaptive differential evolution with combined strategy for global numerical optimization," *Soft Computing*, Vol. 24, No. 9, pp. 6277–6296, May 2020, <https://doi.org/10.1007/s00500-019-03934-3>